


 Cite this: *Chem. Commun.*, 2014, 50, 10438

 Received 14th May 2014,
 Accepted 21st July 2014

DOI: 10.1039/c4cc03649b

www.rsc.org/chemcomm

Group III–V semiconductors are important in the production of a variety of optoelectronic devices. At present, these semiconductors are synthesized by high vacuum techniques. Here we report on the electrochemical deposition of GaN which seems to form in quite a thin layer from NH₄Cl and GaCl₃ in an ionic liquid.

Gallium nitride (GaN) is a semiconducting material which is intensively studied for its use as thin films in optoelectronics (LEDs, laser diodes),^{1,2} electronics (high-power and high frequency devices),^{3,4} as well as sensors.^{5,6} Most technological applications rely on wafer based growth processes which are typically performed in well-defined environments, such as ultra-high vacuum for molecular beam epitaxy in inert atmosphere, or by metal–organic chemical vapour deposition reactors.^{7–9} The low-temperature and low-cost synthesis of gallium nitride nanostructures would be important to make widespread applications and devices. A post-synthesis nitridation of Ga based materials at elevated temperatures in NH₃ atmosphere is one of the possible ways to produce GaN.¹⁰ Another approach includes N₂ or NH₃–H₂ plasma processes, which have been applied to develop III–V semiconductor materials.¹¹ N_x⁺ ion bombardment has also been used to synthesise GaN.¹² There are only a few theoretical and experimental studies on the electrochemical deposition of GaN.^{13–16} In these studies GaN thin films were deposited on SnO₂-coated glass substrates,¹³ Si substrates^{14–16} and indium tin oxide (ITO) coated glass substrates¹⁶ from the mixture of gallium nitrate and ammonium nitrate in deionized water at 20 °C by passing a high voltage between two electrodes. However, there seem to be no follow-up papers.

In this letter, we report on the possible electrochemical synthesis of GaN from the 1-butyl-1-methylpyrrolidinium bis(trifluoromethylsulfonyl)amide ([Py_{1,4}]Tf₂N) ionic liquid containing NH₄Cl and GaCl₃. It was found that NH₄Cl and GaCl₃ form a complex with

the ionic liquid that can be reduced electrochemically at room temperature to form the semiconductor compound, at least in thin layers.

Fig. 1 represents the electrochemical behaviour of [Py_{1,4}]Tf₂N (a) pure, (b) saturated with (~0.05 M) NH₄Cl, (c) containing 0.2 M GaCl₃, and (d) containing a mixture of 0.2 M GaCl₃ and 0.2 M NH₄Cl on copper substrate during cathodic polarization at

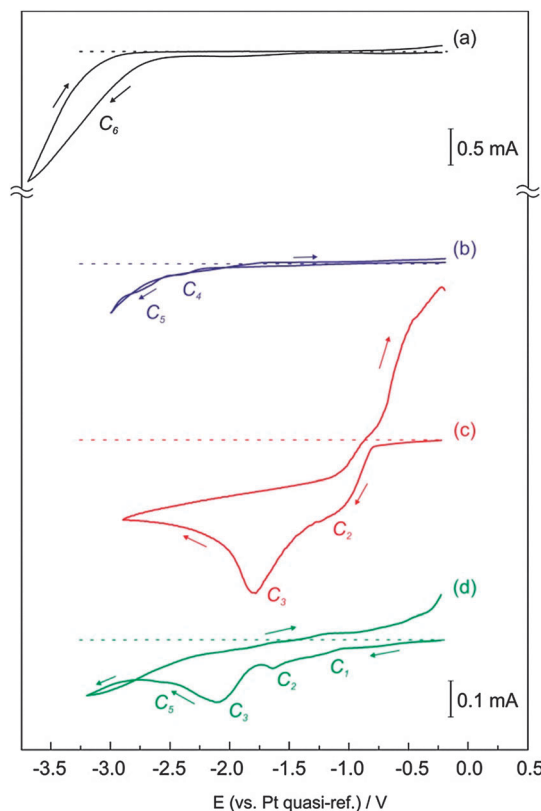


Fig. 1 Comparison of cyclic voltammograms of [Py_{1,4}]Tf₂N ionic liquid (a) pure, (b) saturated with NH₄Cl, (c) containing 0.2 M GaCl₃, and (d) containing a mixture of 0.2 M GaCl₃ and 0.2 M NH₄Cl on copper at room temperature. The scan rate was 10 mV s⁻¹.

*Institute of Electrochemistry, Clausthal University of Technology,
 Arnold-Sommerfeld-Str 6, 38678 Clausthal-Zellerfeld, Germany.*

E-mail: natalia.borisenko@tu-clausthal.de

† Electronic supplementary information (ESI) available: Details of experiment, Raman and IR spectra, and current-time plot. See DOI: 10.1039/c4cc03649b



room temperature. In the case of $[\text{Py}_{1,4}]\text{Tf}_2\text{N}$ saturated with NH_4Cl (Fig. 1b) two weak reduction processes at -2.5 V vs. Pt (C_4) and -2.7 V (C_5) are obtained. These processes must be correlated with the reduction of NH_4^+ ions and the cathodic breakdown of the Tf_2N^- ion,¹⁷ respectively. Beyond -3.1 V, an irreversible reduction of the $[\text{Py}_{1,4}]^+$ ion is observed (C_6 , Fig. 1a). Upon addition of 0.2 M GaCl_3 in $[\text{Py}_{1,4}]\text{Tf}_2\text{N}$, two main reduction processes (C_2 , C_3) appear (Fig. 1c). A broad process between -1.2 V and -1.6 V (C_2) could be attributed to the formation of Cu–Ga alloy, while C_3 corresponds to the three electron reduction process to Ga metal. A similar CV was obtained on Au(111) as shown previously by Gasparotto *et al.*¹⁸ In the anodic regime, an increase in current at -1.0 V is attributed to the oxidation of the electrodeposit. As copper was used as a working electrode, dissolution of Cu can occur at electrode potentials more positive than -0.5 V vs. Pt, leading to the increase in the current. Therefore, all the CV scans were stopped at open circuit potential (OCP) in the anodic regime prior to any copper bulk oxidation.

The electrochemical behaviour changes significantly if NH_4Cl is added to the GaCl_3 -containing ionic liquid (Fig. 1d). A series of reduction processes (C_1 – C_3 , C_5) are obtained prior to the irreversible reduction of the organic cation. Similar to the GaCl_3 -containing $[\text{Py}_{1,4}]\text{Tf}_2\text{N}$, the first two processes (C_1 and C_2) are correlated with the formation of a Cu–Ga alloy and bulk Ga deposition, respectively. We should mention that the dissolution of NH_4Cl in the pure ionic liquid is not more than 0.05 M. However, in the presence of GaCl_3 , about 0.2 M NH_4Cl can be dissolved in the ionic liquid. Raman measurements revealed that an ammonium tetragalliumchloride type complex ($\text{NH}_4^+\text{GaCl}_4^-$) is obtained if both NH_4Cl and GaCl_3 are present in $[\text{Py}_{1,4}]\text{Tf}_2\text{N}$. The third peak C_3 must be attributed to the reduction of the $\text{NH}_4^+\text{GaCl}_4^-$ complex to form Ga and GaN as in this potential regime the formation of a thick layer is clearly seen. C_5 is presumably attributed to the breakdown of the organic anion. In the anodic scan, a rise in the current is seen above -0.8 V due to the oxidation of the electrodeposited product.

Fig. 2 compares Raman (a) and infrared (IR) (b) spectra of pure $[\text{Py}_{1,4}]\text{Tf}_2\text{N}$ (IL) and of $[\text{Py}_{1,4}]\text{Tf}_2\text{N}$ containing NH_4Cl or/and GaCl_3 . Changes in the Raman spectra could only be observed between 0 and 450 cm^{-1} and therefore in Fig. 2a only this region has been emphasised. In the case of the pure IL (black line, Fig. 2a) and NH_4Cl dissolved in the IL (green line, Fig. 2a) the Raman spectra overlap almost perfectly. This is not surprising as it was observed that NH_4Cl does not dissolve more than 0.05 M in the employed ionic liquid. The main peaks between 0 and 500 cm^{-1} are from the Tf_2N^- anion consistent with literature data.¹⁹ If 0.2 M GaCl_3 is added to the IL (red line, Fig. 2a) a peak at 365 cm^{-1} and a shoulder at 140 cm^{-1} appear besides the IL peaks. These are assigned to the GaCl_3 symmetric stretching.²⁰ On addition of NH_4Cl to the GaCl_3 -containing IL (blue line, Fig. 2), a decrease in intensities of the 365 and 140 cm^{-1} peaks are observed. Besides, an additional peak at 152 cm^{-1} , and a peak shift and growth at 342.5 cm^{-1} are obtained. The decrease in intensity of the 365 cm^{-1} peak, the increase in the intensity of the 342.5 cm^{-1} and the formation of an additional peak at 152 cm^{-1} can be attributed to the formation of an $\text{NH}_4^+\text{GaCl}_4^-$

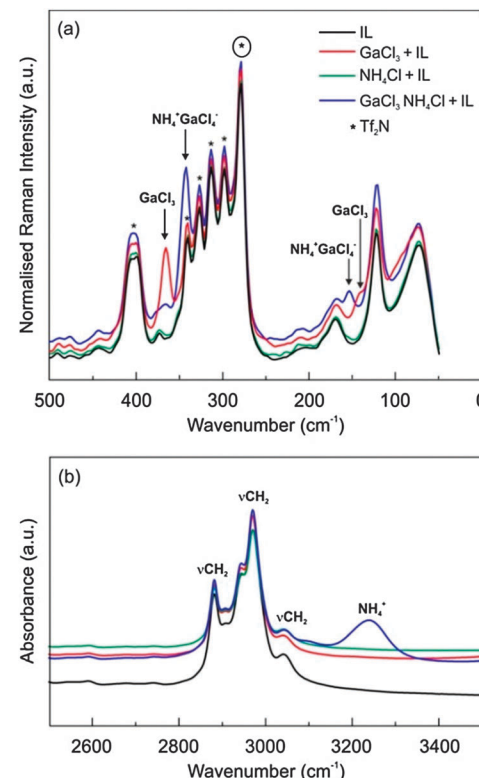


Fig. 2 (a) Raman spectra of IL (black), $\text{GaCl}_3 + \text{IL}$ (red), $\text{NH}_4\text{Cl} + \text{IL}$ (green) and $\text{GaCl}_3, \text{NH}_4\text{Cl} + \text{IL}$ (blue). The Raman spectra was normalised at 278 cm^{-1} (with the small y-axes offset) represented by a circle; (b) IR spectra of these electrolytes.

type complex. Such changes in the Raman spectra have been observed previously in ether/water based solutions for the extraction of GaCl_3 .²¹ However, the presence of the NH_4^+ ion which should be seen between 3030 and 3335 cm^{-1} (ref. 22) was not observed, possibly due to the influence of the $[\text{Py}_{1,4}]$ ion. The complete Raman and infrared spectra are shown in Fig. S1 and S2, ESI.† However, a prominent NH_4^+ peak (Fig. 2b) could be observed in the infrared spectra at 3237 cm^{-1} ,²² thus substantiating the formation of the $\text{NH}_4^+\text{GaCl}_4^-$ type complex in the ionic liquid.

In order to deposit GaN, a constant potential electrodeposition was performed on copper. Fig. 3a and b compares the microstructure of Ga and of GaN in the presence of NH_4Cl made at -2.1 V and -2.5 V, respectively.

Both gallium (Fig. 3a) and GaN made in the presence of NH_4Cl (Fig. 3b) show a spherical morphology with particle sizes ranging between 50 nm and $1\text{ }\mu\text{m}$, consistent with previously published results.¹⁸ Furthermore, the particle density in Fig. 3b is lower compared to that in Fig. 3a. During the electrodeposition of Ga in the presence of NH_4Cl , the current-time plot shows a lot of “noise” indicating the evolution of gaseous species (Fig. S3, ESI†), whereas a smooth curve is observed when electrodepositing Ga alone.

Fig. 4 represents the XRD patterns of the electrodeposits in comparison with GaN powder purchased from Sigma Aldrich. The XRD pattern of the electrodeposited gallium (blue line, Fig. 4) shows the formation of a copper–gallium alloy (CuGa_2 , ICDD 25–275).



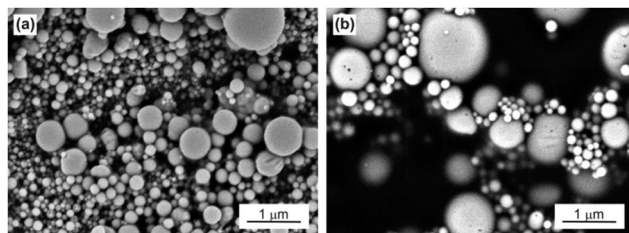


Fig. 3 SEM micrographs of (a) Ga deposited electrochemically at -2.1 V ; (b) GaN electrodeposited at -2.5 V .

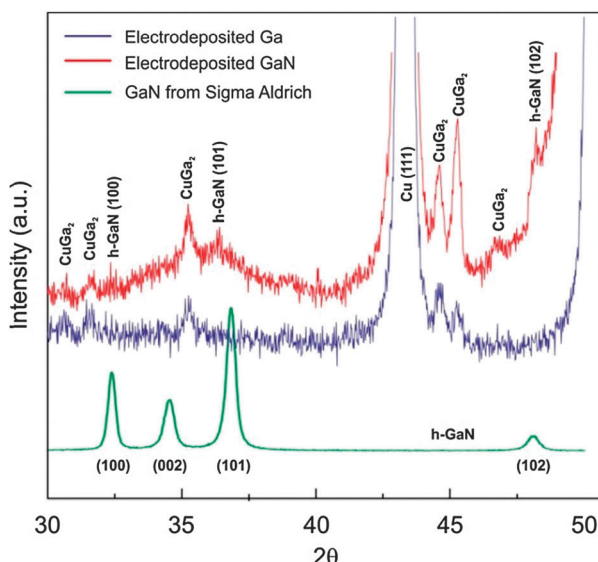


Fig. 4 XRD patterns of the electrodeposited Ga (blue line), GaN (red line) and GaN powder obtained from Sigma-Aldrich (green line).

In comparison, the electrodeposited Ga in the presence of NH_4Cl shows extra peaks at 36.41° and 48.21° (red line, Fig. 4). These two peaks correspond to the formation of GaN (101) and GaN (102). Also, an overall increase in the baseline of the XRD pattern between 32° and 40° is observed which could be due to the partial amorphous nature of deposited GaN. Such broad peak in amorphous GaN was reported recently.²³ We also compared the XRD pattern with commercially available GaN (99.99% purity) from Sigma-Aldrich (green line, Fig. 4). Four peaks between 30° and 50° are observed.

Two peaks of the electrodeposited GaN, namely GaN (101) and GaN (102), are consistent with the GaN obtained from Sigma-Aldrich. However, we find that the main intensity peak of GaN (101) is shifted by 0.4° in the electrodeposited GaN. This might be due to either strain within the GaN or due to doping in the GaN.^{24,25} As in the case of the electrodeposited GaN, the formation of CuGa₂ alloy

took place, therefore there are possibilities that both strain and doping has affected the GaN electrodeposit.

In summary, we have shown that GaN forms if Ga is electrodeposited from GaCl_3 in the presence of NH_4Cl from an ionic liquid at room temperature. Raman and IR spectroscopy reveal that an ammonium chloride-gallium chloride type complex ($\text{NH}_4^+\text{GaCl}_4^-$) is formed when both NH_4Cl and GaCl_3 are present in $[\text{Py}_{1,4}]\text{Tf}_2\text{N}$. Cyclic voltammetry and constant potential deposition showed that this species could be reduced to obtain GaN. The morphology of the GaN was found to be spherical. From XRD, we could show the formation of GaN in the electrodeposit.

Notes and references

- 1 S. C. Jain, M. Willander, J. Narayan and R. Van Overstraeten, *J. Appl. Phys.*, 2000, **87**, 965–1006.
- 2 F. A. Ponce and D. P. Bour, *Nature*, 1997, **386**, 351–359.
- 3 O. Ambacher, *J. Phys. D: Appl. Phys.*, 1998, **31**, 2653–2710.
- 4 S. N. Mohammad and H. Morkoç, *Prog. Quantum Electron.*, 1996, **20**, 361–525.
- 5 M. Stutzmann, G. Steinhoff, M. Eickhoff, O. Ambacher, C. E. Nebel, J. Schalwig, R. Neuberger and G. Müller, *Diamond Relat. Mater.*, 2002, **11**, 886–891.
- 6 S. J. Pearton, F. Ren, Y.-L. Wang, B. H. Chu, K. H. Chen, C. Y. Chang, W. Lim, J. Lin and D. P. Norton, *Prog. Mater. Sci.*, 2010, **55**, 1–59.
- 7 M. M. Sung, C. Kim, S. H. Yoo, C. G. Kim and Y. Kim, *Chem. Vap. Deposition*, 2002, **8**, 50–52.
- 8 S. Strite and H. Morkoc, *J. Vac. Sci. Technol., B: Microelectron. Process. Phenom.*, 1992, **10**, 1237–1266.
- 9 N. Grandjean, J. Massies, Y. Martinez, P. Vennegues, M. Leroux and M. Lägt, *J. Cryst. Growth*, 1997, **3**, 220–228.
- 10 S. Kruckowski, P. Kempisty and P. Strak, *Cryst. Res. Technol.*, 2009, **44**, 1038–1046.
- 11 M. Naddaf, S. S. Hullavarad, V. Ganesan and S. V. Bhoraskar, *Plasma Sources Sci. Technol.*, 2006, **15**, 33–36.
- 12 J. D. Hecht, F. Frost, T. Chassé, D. Hirsch, H. Neumann, A. Schindler and F. Bigl, *Appl. Surf. Sci.*, 2001, **179**, 196–202.
- 13 R. K. Roy and A. K. Pal, *Mater. Lett.*, 2005, **59**, 2204–2209.
- 14 K. Al-Heuseen and M. R. Hashim, *J. Cryst. Growth*, 2011, **324**, 274–277.
- 15 K. Al-Heuseen, M. R. Hashim and N. K. Ali, *Mater. Lett.*, 2010, **64**, 1604–1606.
- 16 K. Al-Heuseen and M. R. Hashim, *AIP Conf. Proc.*, 2012, **1476**, 127–130.
- 17 R. Atkin, S. Zein El Abedin, R. Hayes, L. H. S. Gasparotto, N. Borisenko and F. Endres, *J. Phys. Chem. C*, 2009, **113**, 13266–13272.
- 18 L. H. S. Gasparotto, N. Borisenko, O. Höfft, R. Al-Salman, W. Maus-Friedrichs, N. Bocchi, S. Zein El Abedin and F. Endres, *Electrochim. Acta*, 2009, **55**, 218–236.
- 19 T. Fujimori, K. Fujii, R. Kanzaki, K. Chiba, H. Yamamoto, Y. Umebayashi and S.-I. Ishiguro, *J. Mol. Liq.*, 2007, **131**–132, 216–224.
- 20 J. R. Durig and K. K. Chatterjee, *J. Mol. Struct.*, 1982, **95**, 105–116.
- 21 K. Schug and L. I. Katzin, *J. Phys. Chem.*, 1962, **66**, 907–910.
- 22 G. Socrates, *Infrared and Raman Characteristic Group Frequencies: Tables and Charts*, John Wiley & Sons, West Sussex, England, 3rd edn, 2001.
- 23 H. Z. Xi, B. Y. Man, C. S. Chen, M. Liu, J. Wei and S. Y. Yang, *Semicond. Sci. Technol.*, 2009, **24**, 085024.
- 24 V. Ganesh, S. Suresh, E. Celasco and K. Bhaskar, *Appl. Nanosci.*, 2012, **2**, 169–176.
- 25 S. J. Lee, C. S. Kim, S. K. Noh, K. S. Chung and K. S. Lee, *J. Korean Phys. Soc.*, 2007, **51**, 1050–1054.